

- samples. In July 1988, these chironomids comprised 79% of 2608 arthropods counted in seven larger samples of *Cladophora* turf (M. E. Power, *Oikos*, in press). Because invertebrates concentrate in *Cladophora* (densities, per area projected to the river surface, in algal samples were 29.2 to 41.1 times those in gravel samples) and because algal turfs cover 10 to 30% of the riverbed during summer, tuft-weaving midges are numerically dominant members of the river community at large. Their potential negative effect on *Cladophora* is indicated by results from an experiment in which 5 g (damp weight) of *Cladophora* were placed in small enclosures with 1-mm mesh walls, which are transparent to midge immigration. After 20 days of incubation, *Cladophora* weight (Y, grams damp weight) was negatively related to midge densities (individuals per enclosure): $Y = -0.11X + 4.81$, SE of slope = 0.048, $n = 48$, $P < 0.005$. In experimental outdoor channels, chironomid larvae enhanced export of algae [E. Eichenberger and A. Schlatter, *Verh. Int. Verein. Theoret. Angew. Limnol.* **20**, 1806 (1978)].
8. Cages were 3 m long by 2 m wide by 1.3 m high, and were constructed from plastic screen lined with black plastic shade cloth with a 3-mm mesh. Walls were flared outward at the top to reduce shading and to enhance stability. The shade cloth lining extended 60 cm below the bottom edge of the wall. This "skirt" was buried under gravel in order to anchor the cage and to preclude passage by large fish. Otherwise, the 6-m² enclosed riverbed was unmodified. Drift deflectors of aluminum flashing placed upstream and periodic cleaning prevented drifting detritus from clogging cage walls, which remained transparent to most stream invertebrates and fish fry throughout the 6-week experiment.
 9. Standard length (SL) measures from the anterior end of the head to the center of the crease formed by bending the caudal peduncle [K. F. Lagler, J. E. Bardach, R. R. Miller, D. R. M. Passino, *Ichthyology* (Wiley, New York, ed. 2, 1977), p. 403].
 10. Combined trapping and electroshocking efforts in the study reach from 4 to 6 June 1989 yielded 427 roach, 186 juvenile steelhead, 41 juvenile coho, and 1 gravid female stickleback.
 11. Estimates from snorkeling and shocking (4 to 10 June 1989, before appearance of roach and stickleback fry) ranged from 0.1 to 0.5 individual fish per square meter over an 800-m reach that included riffle and pool habitats. In a September shocking census of a nearby, 117-m² pool, combined densities of roach and steelhead were estimated at 1.26 individuals per square meter [L. R. Brown and P. B. Moyle, *Eel River Survey: Third Year Studies* (Report to the California Department of Fish and Game, Sacramento, 1989)].
 12. Where cross-stream transects intercepted boulder or bedrock, the only substrates supporting macroscopically conspicuous attached algae, I sampled the algae by recording at 10-cm intervals the dominant and subdominant taxa, algal height, condition, and density. Algal height was measured as the modal height of filaments at the sampled site. See M. E. Power and A. J. Stewart [*Am. Midl. Nat.* **117**, 333 (1987)] for methodological details.
 13. Algae and associated biota on bedrock were sampled at 1.0-m intervals where longitudinal transects intercepted boulder or bedrock substrates.
 14. Proportions (SE in parentheses) in six enclosures of 23 to 48 sites with webbed *Cladophora*, uncolonized *Cladophora* turf, and deposited *Nostoc* were 0.72 (0.08), 0.27 (0.08), and 0.01 (0.004), respectively. In the six enclosures, these proportions were 0.07 (0.03), 0.79 (0.05), and 0.15 (0.04), respectively. Average proportions of sites with webbed *Cladophora* differed between enclosures and enclosures [$t = 7.15$, $df = 10$, P (two-tailed) $<< 0.001$]. Before the t test was performed, proportions were arcsin log root-transformed [J. Zar, *Biostatistical Analysis* (Prentice-Hall, Englewood Cliffs, NJ, 1984), p. 241].
 15. Standing crops of attached *Cladophora* sampled from nearby open river sites were similar to standing crops inside all cages at the onset of experiments, and intermediate between standing crops in enclosures and enclosures after 5 weeks. On 5 June, standing crops (milligrams per square centimeter damp weight) from open sites, enclosures, and enclosures were [\bar{x} (SE, n): 298.92 (54.43, 9), 286.37 (141.55, 6), and 265.57 (70.56, 6), respectively. On 16 July, these standing crops were 98.13 (18.08, 8), 33.6 (10.76, 6), and 195.49 (79.81, 6), respectively.
 16. *Cladophora* was brought into the laboratory, where filaments were gently teased apart and all invertebrates >1 mm long were removed, with the exception of cryptic ceratopogonid larvae, which had the diameter and color of *Cladophora* filaments. Cleaned samples were inspected under $\times 10$ magnification, then damp-weighted, and stocked in the stream in 12.7-liter plastic buckets.
 17. S. J. Fretwell, *Perspect. Biol. Med.* **20**, 169 (1977); N. G. Hairston, F. E. Smith, L. B. Slobodkin, *Am. Nat.* **94**, 421 (1960).
 18. L. Floener and H. Bothe, in *Endocytobiology: Endosymbiosis and Cell Biology*, W. Schwemmler and H. E. A. Schwenk, Eds. (de Gruyter, Berlin, 1980), vol. 1, pp. 514–552; J. C. Marks, thesis, Bowling Green State University, Bowling Green, OH (1990).
 19. G. W. Fairchild, R. L. Lowe, W. B. Richardson, *Ecology* **66**, 465 (1985); G. W. Fairchild and R. L. Lowe, *Hydrobiologia* **114**, 29 (1984); V. H. Smith, *Science* **221**, 669 (1983). Drip experiments have demonstrated nitrogen limitation in *Cladophora* during July in the study reach (M. E. Power, unpublished data).
 20. B. A. Menge and J. P. Sutherland, *Am. Nat.* **110**, 351 (1976); *ibid.* **130**, 730 (1987); T. W. Schoener, *Ecology* **70**, 1559 (1989).
 21. Of 21 steelhead sampled, only 7 had any chironomids in their guts: 4 had one chironomid, 1 had two, 1 had four, and 1 had five. Of 46 large roach sampled, only 5 contained any chironomids: 3 had one, 1 had three, and 1 had seven.
 22. D. R. Oliver, *Annu. Rev. Entomol.* **16**, 211 (1971).
 23. R. E. Jones, *Austr. J. Zool.* **22**, 71 (1974).
 24. C. W. Osenberg and G. G. Mittelbach, *Ecol. Monogr.* **59**, 405 (1989); G. G. Mittelbach, *Ecology* **62**, 1320 (1981); W. J. O'Brien, N. A. Slade, G. L. Vinyard, *ibid.* **57**, 1304 (1976).
 25. L. C. V. Pinder, *Annu. Rev. Entomol.* **31**, 1 (1986).
 26. B. A. Menge and A. M. Olson, *Trends Ecol. Evol.* **5**, 52 (1990).
 27. L. Oksanen, *Am. Nat.* **131**, 424 (1988); _____, S. D. Fretwell, J. Arruda, P. Niemela, *ibid.* **118**, 240 (1981).
 28. B. A. Whitton, *Water Res.* **4**, 457 (1970).
 29. S. G. Fisher, L. G. Gray, N. B. Grimm, D. E. Busch, *Ecol. Monogr.* **52**, 93 (1982); J. K. Jackson and S. G. Fisher, *Ecology* **67**, 629 (1986); M. E. Power, *Oikos* **58**, 67 (1990).
 30. I thank B. Harvey and W. Dietrich for discussion; J. Nielsen, P. Steel, T. Steel, H. Kifle, S. Grimm, S. Kupferberg, B. Rainey, S. Kelty, P. Whiting, B. Harvey, and W. Dietrich for help with fieldwork; and W. Getz, T. Schoener, A. Worthington, J. Marks, S. Kupferberg, W. Dietrich, R. B. Hanson, and an anonymous reviewer for comments on the manuscript. This research was supported by NSF grant RII-8600411 and the California State Water Resource Center (W-726).

10 April 1990; accepted 25 July 1990

Sequence-Specific Binding of Human Ets-1 to the T Cell Receptor α Gene Enhancer

I-CHENG HO, NARAYAN K. BHAT, LISA R. GOTTSCHALK, TULLIA LINDSTEN, CRAIG B. THOMPSON, TAKIS S. PAPAS, JEFFREY M. LEIDEN*

Expression of the human T cell receptor (TCR) α gene is regulated by a T cell-specific transcriptional enhancer that is located 4.5 kilobases (kb) 3' to the $C\alpha$ gene segment. The core enhancer contains two nuclear protein binding sites, $T\alpha 1$ and $T\alpha 2$, which are essential for full enhancer activity. $T\alpha 1$ contains a consensus cyclic adenosine monophosphate (cAMP) response element (CRE) and binds a set of ubiquitously expressed CRE binding proteins. In contrast, the transcription factors that interact with the $T\alpha 2$ site have not been defined. In this report, a λ gt11 expression protocol was used to isolate a complementary DNA (cDNA) that programs the expression of a $T\alpha 2$ binding protein. DNA sequence analysis demonstrated that this clone encodes the human *ets-1* proto-oncogene. Lysogen extracts produced with this cDNA clone contained a β -galactosidase-Ets-1 fusion protein that bound specifically to a synthetic $T\alpha 2$ oligonucleotide. The Ets-1 binding site was localized to a 17-base pair (bp) region from the 3' end of $T\alpha 2$. Mutation of five nucleotides within this sequence abolished both Ets-1 binding and the activity of the TCR α enhancer in T cells. These results demonstrate that Ets-1 binds in a sequence-specific fashion to the human TCR α enhancer and suggest that this developmentally regulated proto-oncogene functions in regulating TCR α gene expression.

MAMMALIAN T LYMPHOCYTES CAN be divided into two subsets on the basis of their expression of distinct heterodimeric cell-surface antigen receptor molecules (1). Greater than 90% of peripheral blood T cells, including cells of the helper and cytotoxic phenotypes, express the disulfide-linked α/β T cell receptor (TCR). In contrast, 2 to 10% of circulating

I-C. Ho, L. R. Gottschalk, C. B. Thompson, J. M. Leiden, Howard Hughes Medical Institute and Departments of Internal Medicine and Microbiology/Immunology, University of Michigan Medical School, Ann Arbor, MI 48109.
N. K. Bhat and T. S. Papas, Laboratory of Molecular Oncology, National Cancer Institute, Frederick, MD 21701.
T. Lindsten, Department of Pathology, University of Michigan Medical School, Ann Arbor, MI 48109.

*To whom correspondence should be addressed.

T cells of unknown function express the related, but distinct, γ/δ TCR (2, 3). Each of the TCR genes is composed of multiple germ line gene segments that rearrange during thymocyte ontogeny to form mature antigen receptor genes (3). The TCR gene rearrangements are generally restricted to cells of the T lymphocyte lineage and may be regulated by transcription of the unrearranged TCR loci (4). Thus, a better understanding of the mechanisms that regulate TCR transcription might also yield insights into molecular mechanisms that regulate T lymphocyte development.

Expression of the human and murine TCR α genes is regulated by highly related transcriptional enhancers located 4.5 kb 3' to the C α gene segments (5, 6). The human TCR α enhancer is required for high-level transcription from a TCR V α (V, variable gene segment) promoter and is active only in TCR α/β^+ T cells (6). The core enhancer has been localized to a 116-bp fragment that contains two nuclear protein binding sites, T α 1 and T α 2, both of which are required for full enhancer activity (6). T α 1 contains a consensus cAMP response element (CRE) and binds a set of ubiquitously expressed CRE binding proteins (7). In contrast, although T α 2 binds in a sequence-specific fashion to protein or proteins present in T cell nuclear extracts (8), the identity of these nuclear proteins has not yet been determined.

We have used a λ gt11 expression protocol (9, 10) to clone cDNAs that encode T α 2 binding proteins. A λ gt11 cDNA library was constructed from Jurkat T cell

polyadenylated (poly(A)⁺) RNA, and ~750,000 recombinant clones were screened with a ³²P-labeled, multimerized, double-stranded T α 2 synthetic oligonucleotide probe. One clone was identified that bound to a T α 2 probe but not to an unrelated control DNA probe (11). DNA sequence analysis demonstrated that this clone contained a 1.9-kb human *ets-1* cDNA that included 58 bp of 5' untranslated region, the entire 1323-bp *ets-1* coding region, and ~520 bp of 3' untranslated region joined in-frame, in a 5' to 3' orientation, to the *Escherichia coli* β -galactosidase gene of λ gt11 (Fig. 1A). The *ets-1* 5' untranslated region contained in this cDNA clone did not include an in-frame stop codon, thus allowing expression of an intact β -galactosidase-Ets-1 fusion protein.

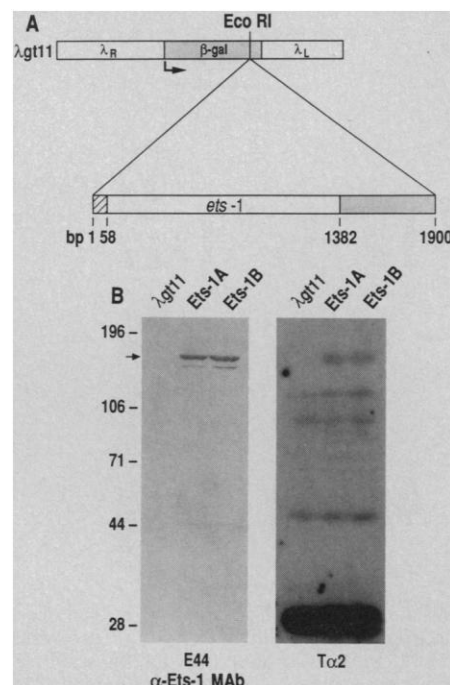
ets-1 is a member of the *c-ets* family of genes (*ets-1*, *ets-2*, *erg*, *elk-1*, *elk-2*, and *PU.1*) that have been identified by sequence similarity to the *v-ets* oncogene of the E26 leukemia virus (12–14). Ets-1 is a nuclear protein that binds to DNA (15) and has recently been reported to bind in a sequence-specific fashion to the long terminal repeat (LTR) of the Moloney murine sarcoma virus (MSV) (16). Although Ets-1 has been shown to be expressed in a lymphoid-specific fashion (17), a function for Ets-1 in the regulation of cellular transcription has not been demonstrated. To confirm the specificity of binding of the β -galactosidase-Ets-1 fusion protein, lysogen extracts from the *ets-1* cDNA clone were used in Southwestern (DNA-protein) blot and electro-

phoretic mobility shift assays. Control λ gt11 lysogen extract and two different Ets-1 lysogen extracts (Ets-1A and Ets-1B) were subjected to electrophoresis, transferred to nitrocellulose, and probed with either monoclonal antibody (MAb) to Ets-1 (anti-Ets-1 MAb) (Fig. 1B, left), or ³²P-labeled T α 2 oligonucleotide (Fig. 1B, right). Both the anti-Ets-1 MAb and the T α 2 oligonucleotide probe bound to a 170-kilodalton (kD) protein that was present in both of the Ets-1 lysogen extracts. This protein was absent from the control λ gt11 lysogen extract. The size of this band corresponded to the expected size of the β -galactosidase-Ets-1 fusion protein, and the same band was detected on duplicate blots probed with an anti- β -galactosidase antiserum (11). Furthermore, this band was not seen in control Southwestern (DNA) immunoblots probed with a T α 1 oligonucleotide (11), confirming the specificity of the Ets-1-T α 2 interaction.

Binding of the Ets-1 fusion protein was also examined by electrophoretic mobility shift assays (Fig. 2). The Ets-1A lysogen extract contained a protein that bound to a ³²P-labeled T α 2 oligonucleotide probe (Fig. 2A), but not to a similarly prepared T α 1 control probe (11). This binding activity was not contained in control λ gt11 lysogen extracts (Fig. 2A), and was inhibited by the addition of unlabeled T α 2 competitor DNA, but not by T α 1 control competitor DNA (Fig. 2B). Evidence that the altered band seen by electrophoretic mobility shift assay was a result of binding of the β -galactosidase-Ets-1 fusion protein was obtained by showing that the mobility of this band was further reduced by treatment of the lysogen extract with anti-Ets-1 MAb, but not by treatment with anti-Ets-2 MAb (control) (Fig. 2A). Moreover, the formation of this complex was inhibited by treatment of the lysogen extract with anti- β -galactosidase antiserum (Fig. 2A) (18). Taken together, these experiments demonstrate that Ets-1 bound to the T α 2 site of the human TCR α enhancer in a sequence-specific fashion.

We next attempted to localize the Ets-1 binding site within the T α 2 domain. Methylation interference suggested that the Ets-1 binding site in the MSV LTR is centered around a 20-bp sequence, 5'-CTCGGAGAGCGGAAGCGCGC-3' (16). The 3' end of the T α 2 binding site as defined by deoxyribonuclease (DNase) I footprint analysis (6) contains two sequences that display significant identity with the MSV LTR Ets-1 binding site, including core sequences that are conserved at 7 of 10 and 8 of 10 bp. In order to determine whether human Ets-1 was capable of binding to these sites, synthetic oligonucleotides (Fig. 3A) were used

Fig. 1. Sequence-specific binding of Ets-1 to the T α 2 site of the human TCR α enhancer. (A) A schematic representation of a λ gt11 cDNA clone that encodes a T α 2 binding protein. A Jurkat cDNA library was constructed in λ gt11, and clones were screened for T α 2 binding as described (9, 10, 28). One clone produced a fusion protein that bound to a multimerized T α 2 oligonucleotide probe, but not to a multimerized control oligonucleotide probe. The 1.9-kb insert from this clone was subjected to DNA sequence analysis and shown to contain a partial length *ets-1* cDNA. The structure of this cDNA is shown schematically in the bottom panel. The 5' untranslated region is depicted by the cross-hatched box, the *ets-1* open reading frame by the open box, and the 3' untranslated region by the shaded box. For the sake of clarity, λ gt11 is depicted with the right arm (λ R) at the left side of the schematic illustration. (B) Immunoblot and Southwestern blot (DNA-to-protein) analyses of the β -galactosidase-Ets-1 fusion protein. Control λ gt11 and two independent *ets-1* lysogens (*ets-1A* and *ets-1B*) were produced in *E. coli* Y1089 as described (9). Lysogen extracts prepared from these clones were fractionated on SDS-polyacrylamide (7%) gels and electrophoretically transferred to nitrocellulose. Duplicate blots were subjected to immunoblot analysis (29) with the E44, anti-Ets-1 MAb (30) (left) and Southwestern blot analysis (31) (right) with a ³²P-labeled, tetrameric T α 2 oligonucleotide probe. Molecular size markers in kilodaltons are shown at the left of the immunoblot.



in electrophoretic mobility shift assays with recombinant Ets-1 protein (Fig. 3B). Ets-1 bound with relatively high affinity to the Tα2a and Tα2c oligonucleotides, both of which contained the more 3' region of similarity to the MSV LTR binding site. In contrast, weak binding of Ets-1, which was only detectable on prolonged autoradiographic exposures, was observed with the Tα2b probe. These experiments demonstrate that the major Ets-1 binding site in the human

TCR α enhancer localizes to a 17-bp sequence at the 3' end of the Tα2 element.

To assess the biological importance of Ets-1 binding to Tα2, the effects of mutations in this site upon Ets-1 binding and TCR α transcriptional enhancer activity were determined (Fig. 4). Five nucleotide substitutions within the core binding site abolished binding of recombinant Ets-1 to a synthetic Tα2c oligonucleotide probe (Fig. 4B). These same mutations were then intro-

duced into the Tα2 site of the minimal human TCR α enhancer. The resulting mutant enhancer was cloned into the pSPCAT reporter plasmid and assayed for enhancer activity after transfection into human Jurkat T cells. Mutation of the Ets-1 binding site decreased enhancer activity by 95%. These results confirmed the localization of the Ets-1 binding site at the 3' end of Tα2 and demonstrate that this site functions in regulating the activity of the TCR α enhancer in T cells.

Ets-1 is a nuclear protein that is expressed preferentially in cells of the T and B lymphocyte lineages (17). Ets-1 expression in thymocytes has been shown to be induced on fetal day 18, the same time that the TCR α gene is rearranged and expressed (19). Moreover, Ets-1 and TCR α mRNA are coordinately increased during the activation of Jurkat T cell tumor cells (20). We have demonstrated that Ets-1 interacts in a sequence-specific fashion with an essential transcriptional regulatory element of the human T cell receptor α enhancer. Taken together, these results strongly suggest an important function for Ets-1 in the regulation of TCR α gene expression during thymocyte ontogeny. It will be important to determine the regions of Ets-1 that are responsible for its DNA binding and transcriptional regulatory activities. An examination of the Ets-1 protein sequence failed to reveal previously defined DNA binding domains such as the leucine zipper, zinc finger, or helix-turn-helix motifs. *ets-1* is a member of a multigene family that includes *ets-2*, *erg*, *elk-1*, *elk-2*, and *PU.1* (12-14). Each of these proteins contains a highly conserved COOH-terminal basic domain linked to a distinct NH₂-terminus. Two lines of evidence suggest that these shared basic domains are important for DNA binding. First, similar but distinct basic domains function in DNA binding in members of the leucine zipper family of transcription factors (21). Second, deletion of the COOH-terminal basic domain from Ets-1 results in the loss of the ability of the molecule to bind to whole calf thymus DNA (15). It also will be important to determine whether members of the *c-ets* family bind to DNA as monomers or, instead, as homo- or heterodimers.

We postulate that the members of the *c-ets* multigene family are transcriptional regulatory proteins that bind to related DNA sequences through a conserved COOH-terminal basic domain and mediate diverse transcriptional regulatory functions with their distinct NH₂-terminal regions. Some of the members of this family, such as *ets-1* and *elk-1*, are expressed in a tissue-specific fashion (14), while others, such as *ets-2*, appear to display a broader range of tissue distribution (22). *ets-2* is not expressed in

Fig. 2. Electrophoretic mobility shift assays of the Ets-1 fusion protein. **(A)** Effects of anti-Ets-1 and anti-β-galactosidase on the DNA binding activity of the Ets-1-β-galactosidase fusion protein. Extracts from control λgt11 lysogens of the Ets-1A lysogen (Fig. 1A) were used in electrophoretic mobility shift assays with a ³²P-labeled tetrameric Tα2 oligonucleotide probe. Prior to the addition of the labeled probe, lysogen extracts (3 μl) were incubated for 30 min at 4°C with no antibody (-), the E44, anti-Ets-1 MAb (α-Ets-1) (1 μl), the U244 anti-Ets-2 MAb (α-Ets-2) (1 μl), or a commercially available affinity-purified rabbit anti-β-galactosidase antiserum (1 μl) (Organon Teknika). Electrophoretic mobility shift assays were performed as described (8). The arrow denotes the specific band of altered mobility that was present in the Ets-1 lysogen extract and reacted with anti-Ets-1 and anti-β-galactosidase. **(B)** Cold competitor analysis of the Ets-1 fusion protein. Extracts from a control λgt11 lysogen or the Ets-1A lysogen were used in electrophoretic mobility shift assays with a ³²P-labeled tetrameric Tα2 oligonucleotide probe in the absence or presence of unlabeled tetrameric Tα1 or Tα2 competitor DNAs.

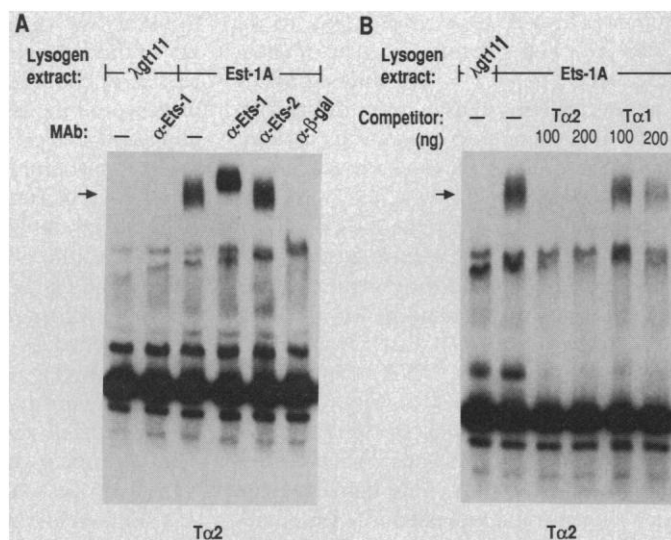
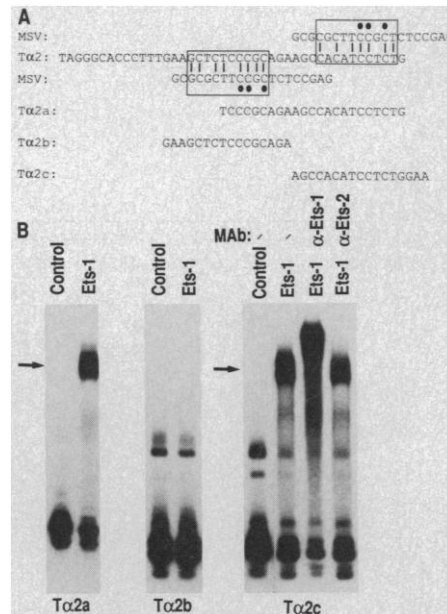


Fig. 3. Localization of the Ets-1 binding site in the human TCR α enhancer. **(A)** Schematic representation of the synthetic oligonucleotides used in electrophoretic mobility shift assays. The sequence of the Tα2 nuclear protein binding site from the human TCR α enhancer (Tα2) (6) is compared to the Ets-1 binding site from the MSV LTR (MSV) (16). Nucleotides in the MSV LTR that are protected from methylation by Ets-1 binding are dotted. Potential Ets-1 binding sites in the Tα2 sequence are boxed. **(B)** Electrophoretic mobility shift analysis of the binding activity of recombinant Ets-1 to different regions of the human TCR α enhancer. Four copies of the wild-type Tα2 oligonucleotide or oligonucleotides Tα2a, Tα2b, or Tα2c were cloned into pUC, end-labeled with [^{α-32}P]dCTP and [^{α-32}P]dGTP as described (8) and used in electrophoretic mobility shift assays as described in the legend to Fig. 2. Recombinant Ets-1 was produced by cloning the full length *ets-1* cDNA into the pTTQ prokaryotic expression vector (33) followed by transformation of *E. coli* DH5α. Bacterial cultures containing pTTQ with (Ets-1) or without (control) the *ets-1* cDNA insert were grown to an OD₆₀₀ of 0.5 and recombinant protein synthesis was induced by the addition of 10 mM isopropylthio-β-D-galactoside for 2.5 hours at 37°C. Bacterial extracts were prepared (9) and 3 μl of extract was used in each electrophoretic mobility shift assay. Experiments performed with anti-Ets-1 (α-Ets-1) or anti-Ets-2 (α-Ets-2) MABs were as described in the legend to Fig. 2. Arrows denote the bands of altered mobility that correspond to Ets-1 protein binding. On prolonged autoradiographic exposures, a faint band of altered mobility was present in the Ets-1 lane with the Tα2b oligonucleotide probe (11).



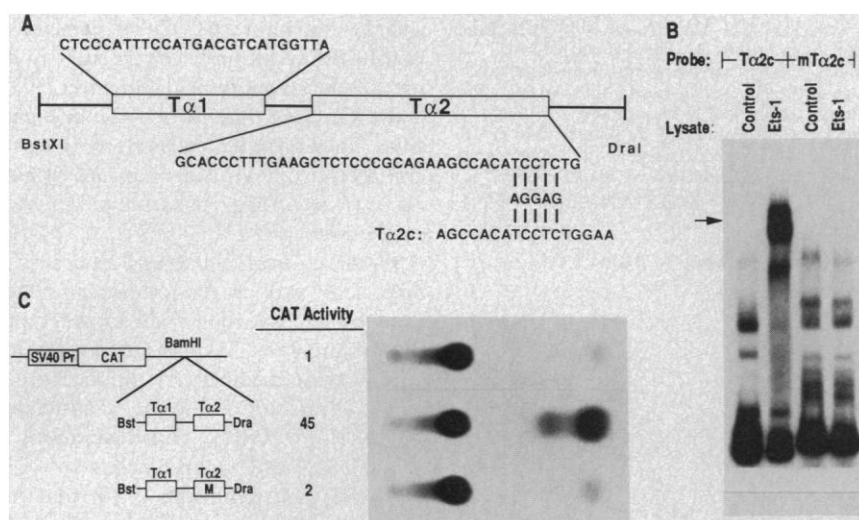


Fig. 4. Effects of mutations of the Ets-1 binding site on TCR α enhancer function. **(A)** Schematic representation of the minimal human TCR α enhancer. The 116-bp Bst XI–Dra I fragment that contains the minimal human TCR α enhancer (6) is shown schematically along with the sequences of the wild-type Ta1 and Ta2 nuclear protein binding sites. The five nucleotide substitutions (AGGAG), which were introduced into both the Ta2c oligonucleotide and the minimal TCR α enhancer, are shown below the map of the enhancer. **(B)** Effects of mutations of the Ets-1 binding site on binding to recombinant Ets-1. Recombinant Ets-1 prepared as described in the legend to Fig. 3 was used in electrophoretic mobility shift assays with 32 P-labeled wild-type (Ta2c) or mutant Ta2c (mTa2c) oligonucleotide probes [see (A)]. Arrows denote the band of altered mobility that corresponded to Ets-1 binding. Control extracts (control) were prepared from cultures of *E. coli* DH5 α that contained the pTTQ expression vector without the *ets-1* cDNA insert. **(C)** Effects of mutations of the Ets-1 binding site on human TCR α enhancer activity. The five nucleotide substitutions within the Ets-1 binding site shown in (A) were introduced into the 116-bp Bst XI–Dra I minimal TCR α enhancer with the polymerase chain reaction (34). The fidelity of mutagenesis was confirmed by dideoxy nucleotide sequence analysis. The wild-type or mutant TCR α enhancer fragments (M) were then cloned into the Bam HI site of the pSPCAT reporter plasmid (35) 3' of the minimal SV40 promoter (SV40Pr) and bacterial chloramphenicol acetyl transferase (CAT) gene. The resulting plasmids were transfected into human Jurkat T cells as described (6). To control for differences in transfection efficiencies, all transfections also contained the pRSV β gal reference plasmid (2 μ g). Cell extracts prepared 48 hours after transfection were assayed for both CAT and β -galactosidase activities as described (8). The data is shown as CAT activities relative to that produced by the enhancerless pSPCAT control plasmid following correction for differences in transfection efficiencies.

resting T cells but is rapidly induced after T cell activation (22). In addition, the transcriptional regulatory domains of several inducible T cell genes, including the interleukin-2 (IL-2) (23), IL-3 (24), IL-4 (25), and granulocyte-macrophage colony-stimulating factor (GM-CSF) (26) genes, contain potential Ets binding sites. Thus, Ets-2 or a related *c-ets* family member might regulate the expression of multiple genes during the process of T cell activation.

The human TCR α enhancer displays T cell-specific activity (6). Because Ets-1 is expressed in both B and T cells, it seems unlikely that Ets-1 alone is responsible for the T cell-specific activity of this enhancer. However, a number of observations suggest that Ets-1 may bind to the Ta2 site in concert with additional transcriptional regulatory proteins. First, the affinity of recombinant Ets-1 alone for monomer Ta2 binding sites is low (11). In addition, the Ta2 DNase I footprint appears to be significantly larger than the minimal Ets-1 binding site (6), and mutations of Ta2 outside the Ets-1 binding site significantly reduce enhancer

activity (8). Finally, preliminary ultraviolet-cross-linking studies have demonstrated that at least two T cell nuclear proteins, one of which corresponds in size to Ets-1, bind to the 3' end of Ta2 (11). Thus, it is possible that Ets-1 binding to the TCR α enhancer is enhanced when Ets-1 is complexed with a second protein. If the expression of the second protein were restricted to T cells, binding of the Ets-1 protein complex might be relatively T cell-specific. Finally, several of the *c-ets* family members map to chromosomal translocation sites that have been implicated in both lymphoid and nonlymphoid malignancies (14, 27). A model of *c-ets* family members as sequence-specific DNA binding proteins with transcriptional regulatory activities may facilitate future studies designed to better understand both their function in normal development and their oncogenic potential.

REFERENCES AND NOTES

- J. L. Strominger, *Science* **244**, 943 (1989).
- P. Marrack and J. Kappler, *ibid.* **238**, 1073 (1987).
- M. M. Davis and P. J. Bjorkman, *Nature* **334**, 395 (1988).

- G. Yancopoulos *et al.*, *Cell* **44**, 251 (1986); T. K. Blackwell *et al.*, *Nature* **324**, 585 (1986).
- A. Winoto and D. Baltimore, *Cell* **59**, 649 (1989).
- I.-C. Ho, L.-H. Yang, G. Morle, J. M. Leiden, *Proc. Natl. Acad. Sci. U.S.A.* **86**, 6714 (1989).
- L. R. Gottschalk and J. M. Leiden, *Mol. Cell. Biol.*, in press.
- I.-C. Ho and J. M. Leiden, *ibid.* **10**, 4720 (1990).
- H. Singh, J. H. LeBowitz, A. S. Baldwin, P. A. Sharp, *Cell* **52**, 415 (1988).
- C. R. Vinson, K. L. LaMarco, P. F. Johnson, W. H. Landschulz, S. L. McKnight, *Genes Dev.* **2**, 801 (1988).
- I.-C. Ho, L. R. Gottschalk, J. M. Leiden, unpublished data.
- E. S. P. Reddy and V. N. Rao, *Oncogene Research* **3**, 239 (1988); D. K. Watson *et al.*, *Proc. Natl. Acad. Sci. U.S.A.* **85**, 7862 (1988).
- V. N. Rao *et al.*, *Science* **237**, 635 (1987).
- V. N. Rao *et al.*, *ibid.* **244**, 66 (1989); M. J. Klemsz *et al.*, *Cell* **61**, 113 (1990).
- K. E. Boulukos, P. Pogoniec, B. Rabault, A. Begue, J. Ghysdael, *Mol. Cell. Biol.* **9**, 5718 (1989); S. Fujiwara *et al.*, *Oncogene* **2**, 99 (1988).
- C. V. Gunther, J. A. Nye, R. S. Bryner, B. J. Graves, *Genes Dev.* **4**, 667 (1990).
- N. K. Bhat *et al.*, *Proc. Natl. Acad. Sci. U.S.A.* **84**, 3161 (1987); N. K. Bhat *et al.*, *J. Immunol.* **142**, 672 (1989); P. Pogoniec *et al.*, *Oncogene* **4**, 691 (1989).
- The difference between the effects of the anti-Ets-1 and anti- β -galactosidase antibodies on recombinant Ets-1 binding is probably due to the fact that the anti- β -galactosidase antibody is a polyclonal antiserum that binds to multiple epitopes of the fusion protein. Binding of one or more of these antibodies to the β -galactosidase protein may in some way alter the conformation or accessibility of the Ets-1 DNA binding domain, thereby interfering with the formation of the Ets-1–DNA complex. In contrast, anti-Ets-1 is a monoclonal reagent directed against a single Ets-1 peptide epitope. Binding of this MAB does not interfere with the DNA binding properties of the β -galactosidase–Ets-1 fusion protein, but rather alters the electrophoretic mobility of the Ets-1–DNA complex.
- H. R. Snodgrass, P. Kiscilow, M. Kiefer, M. Steinmetz, H. von Boehmer, *Nature* **313**, 592 (1985); D. H. Raulat, R. D. Garman, H. Saito, S. Tonegawa, *ibid.* **314**, 103 (1985).
- N. K. Bhat and T. S. Pappas, unpublished data.
- W. H. Landschulz, P. F. Johnson, S. L. McKnight, *Science* **240**, 1759 (1988); *ibid.* **243**, 1681 (1989); M. Neuberger, M. Schuermann, J. B. Hunter, R. Muller, *Nature* **338**, 589 (1989); R. Turner and R. Tjian, *Science* **243**, 1689 (1989).
- N. K. Bhat *et al.*, *Proc. Natl. Acad. Sci. U.S.A.* **87**, 3723 (1990).
- T. Fujita *et al.*, *Cell* **46**, 401 (1986).
- S. Miyatake, T. Yokota, F. Lee, K. Arai, *EMBO J.* **4**, 2561 (1985).
- T. Otsuka *et al.*, *Nucleic Acids Res.* **15**, 33 (1987).
- S. Miyatake *et al.*, *EMBO J.* **4**, 2561 (1985).
- N. Sacchi *et al.*, *Science* **231**, 379 (1986).
- A λ gt11 cDNA library was constructed with random hexanucleotide primers (Invitrogen) and poly(A)⁺ RNA (5 μ g) from Jurkat human T cells stimulated for 16 hours with phorbol myristate acetate (3 ng/ml) and ionomycin (800 ng/ml). 32 P-labeled Ta2 probe for library screening was prepared as described (10) by ligating 2 μ g of phosphorylated, double-stranded oligonucleotides that corresponded to the Ta2 nuclear protein binding site (5'-TAGGGCACCCCTTTGAAGCTCTCCCGCAGAAGCCACATCCTC-3') (6) for 1 hour at 23°C. Multimerized oligonucleotide probe (500 ng) was labeled with [α - 32 P]dGTP and [α - 32 P]dCTP with a commercially available nick translation kit (BRL). Nitrocellulose filters that contained 50,000 recombinant plaques per filter were prepared as described (9) and preincubated for 1 hour at room temperature in BLOTTO-TNE25 [5% Carnation instant milk (Blotto) in 10 mM Tris, pH 7.5, 25 mM NaCl, 1 mM EDTA, 1 mM dithiothreitol] followed by washing twice for 1 min in TNE25. Filters (15) were then incubated with labeled probe (2 \times 10⁶ dpm/ml) in 50 to 75 ml of TNE25 that contained denatured sonicated calf thymus DNA (5

$\mu\text{g/ml}$) for 1 hour at room temperature with gentle shaking. Filters were washed three times for 10 min in TNE25 (250 ml) and were subjected to autoradiography with DuPont intensifying screens.

29. E. Quakenbush *et al.*, *Proc. Natl. Acad. Sci. U.S.A.* **84**, 6526 (1987).

30. S. Koizumi *et al.*, *Oncogene* **5**, 675 (1990).

31. L. M. Staudt *et al.*, *Science* **241**, 577 (1988).

32. S. Fujiwara *et al.*, *Mol. Cell. Biol.* **8**, 4700 (1988).

33. M. J. R. Stark, *Gene* **51**, 255 (1987).

34. M. S. Parmacek and J. M. Leiden, *J. Biol. Chem.* **264**, 13217 (1989).

35. K. Leung and G. J. Nabel, *Nature* **333**, 776 (1988).

36. The authors thank D. Ginsburg and G. Nabel for critical review of the manuscript. We also acknowledge S. Fujiwara and S. Koizumi for providing the anti-Ets MAbs used in these studies. We thank B. Burck for preparation of the illustrations and J. Pickett for expert secretarial assistance. Supported in part by Public Health Service grant AI-29673. T.L. is a Special Fellow of the Leukemia Society of America.

11 May 1990; accepted 31 August 1990

A Map of Visual Space Induced in Primary Auditory Cortex

ANNA W. ROE, SARAH L. PALLAS, JONG-ON HAHM, MRIGANKA SUR*

Maps of sensory surfaces are a fundamental feature of sensory cortical areas of the brain. The relative roles of afferents and targets in forming neocortical maps in higher mammals can be examined in ferrets in which retinal inputs are directed into the auditory pathway. In these animals, the primary auditory cortex contains a systematic representation of the retina (and of visual space) rather than a representation of the cochlea (and of sound frequency). A representation of a two-dimensional sensory epithelium, the retina, in cortex that normally represents a one-dimensional epithelium, the cochlea, suggests that the same cortical area can support different types of maps. Topography in the visual map arises both from thalamocortical projections that are characteristic of the auditory pathway and from patterns of retinal activity that provide the input to the map.

THE MECHANISMS BY WHICH sensory maps form in the neocortex remain an outstanding question in cortical development. There is evidence that both the cortical target tissue (1) and sensory information from peripheral receptors (2) are important in the mapping process. We have addressed the question by using a preparation in which fibers from the retina are directed into the auditory pathway in ferrets. In particular, we asked whether primary auditory cortex, which normally contains a representation of the cochlea, would now contain a systematic map of the retina and of visual space. We reasoned that a map of the visual field in primary auditory cortex, if it were to exist, would also provide important clues to how cortical targets and sensory inputs contribute to generating maps of sensory surfaces in the cortex.

To route visual projections to auditory cortex, the retina is deprived of its two major targets by surgical lesions in neonatal ferret kits. One target, the superior colliculus, is ablated directly, while the other target, the lateral geniculate nucleus (LGN), atrophies severely by retrograde degenera-

tion after ablation of visual cortex. Concurrently, ascending auditory fibers to the medial geniculate nucleus (MGN), the principal auditory thalamic nucleus, are sectioned in the brachium of the inferior colliculus. Retinal afferents then project into the deaf-ferented MGN (3); in lesioned animals reared to adulthood, neurons with well-defined visual responses can be recorded in this nucleus and from its main cortical target, the primary auditory cortex (4).

We have now examined the map of the visual field induced in primary auditory cortex in lesioned animals. Adult ferrets ($n = 7$), operated on at birth as described above, were prepared for electrophysiological recording (5). A grid of electrode penetrations was made in primary auditory cortex. We plotted receptive fields of visual cells recorded in cortex on a tangent screen using flashing or moving spots or bars of light. We identified recording sites as lying within primary auditory cortex by matching lesions made during recording with borders defined histologically (6).

Cortical recording sites and corresponding visual receptive field locations from an adult ferret in which retinal projections were induced into the auditory pathway are shown in Fig. 1. Receptive fields close to the vertical midline of the visual field are represented at the medial edge of primary auditory cortex (Fig. 1, A to C; receptive fields 1

and 2), and more peripheral parts of the visual field lie progressively laterally in cortex. Several receptive field sequences (Fig. 1, B and C) show that lower visual field elevations are represented posteriorly in cortex, and receptive fields move upward in elevation as recording sites move anteriorly across cortex.

We have quantified several aspects of the map. The map is retinotopic overall, although there is some variability in receptive field location (7). Azimuths increase systematically with mediolateral distance on the cortex (Pearson's coefficient of correlation, $r = 0.74$, $P < 0.01$), while elevations increase from posterior to anterior ($r = 0.46$, $P < 0.05$). Mapping indices (7) that compare actual locations with theoretical ones for a perfectly retinotopic map indicate that azimuths are mapped more precisely than elevations (8). Magnification (9) is relatively constant across the map (Fig. 1D), suggesting a linear mapping of the retina on cortex (10).

The map shown in Fig. 1 is an example of the maps we have recorded in primary auditory cortex in four lesioned animals. The representation of azimuth is stereotypical in all maps, increasing from medial to lateral in cortex. Furthermore, the representation of azimuth is consistently more precise than the representation of elevation (11). Indeed, the polarity of the elevation representation can reverse in some animals so that elevations either increase from posterior to anterior in cortex (as shown in Fig. 1; three animals) or from anterior to posterior (data not shown; one animal).

We regard these observations as significant for understanding how sensory maps form in the cortex. Our results demonstrate that the form of the map is not an intrinsic property of the cortex and that a cortical area can come to support different types of maps. In normal ferrets, primary auditory cortex contains a representation of the cochlea (12), with low sound frequencies represented laterally and high frequencies medially in cortex; the mediolateral dimension thus constitutes the variable-frequency axis in cortex. Neurons along the anteroposterior dimension in primary auditory cortex all represent the same sound frequency and constitute the isofrequency axis (13). In lesioned ferrets, a systematic representation of the retina and of visual space occupies both the mediolateral and anteroposterior dimensions of cortex. Thus, cortex that normally represents a one-dimensional (1-D) sensory epithelium (the cochlea) can, after early developmental manipulations, represent topographically a two-dimensional (2-D) epithelium (the retina).

The mechanisms by which topography is

Department of Brain and Cognitive Sciences, Massachusetts Institute of Technology, Cambridge, MA 02139.

*To whom correspondence should be addressed at Department of Brain and Cognitive Sciences, E25-618, Massachusetts Institute of Technology, Cambridge, MA 02139.